IEEE Access
Multidisciplinary | Rapid Review | Open Access Journal

Received March 27, 2020, accepted April 20, 2020, date of publication April 23, 2020, date of current version May 6, 2020.

Digital Object Identifier 10.1109/ACCESS.2020.2989804

Exploiting Temporal Correlation Mechanism for Designing Temperature-Aware Energy-Efficient Routing Protocol for Intrabody Nanonetworks

SHUMAILA JAVAID[1], ZHENQIANG WU[1], HAMZA FAHIM[2], MIAN MUHAMMAD SADIQ FAREED[3], AND FARHANA JAVED[4]

[1]School of Computer Science, Shaanxi Normal University, Xi'an 710119, China
[2]School of Electronics and Information, Xi'an Jiaotong University, Xi'an 710049, China
[3]Guangxi Key Laboratory of Embedded Technology and Intelligent System, Guilin University of Technology, Guilin 541004, China
[4]Department of Network Engineering, Universitat Politècnica de Catalunya (UPC), 08028 Barcelona, Spain

Corresponding authors: Shumaila Javaid (shumaila@snnu.edu.cn) and Zhenqiang Wu (zqiangwu@snnu.edu.cn)

This work was supported by the National Natural Science Foundation of China under Grant 61962033, and in part by the Xi'an Key Laboratory of Mobile Edge Computing and Security under Grant 201805052-ZD3CG36.

ABSTRACT An Intrabody Nanonetwork (IBNN) is composed of integrated nanoscale devices, implanted inside the human body to collect diagnostic information and tuning medical treatments. The non-invasive continuous monitoring and precision of these nanoscale devices in the diagnostic of diverse diseases is improving advanced monitoring, therapeutic, and telemedicine services. The unique feature constraints of these nanoscale devices (such as inadequate energy, storage, and computational resources) along with the molecular absorption thermal challenges due to Electromagnetic (EM) communication in the Terahertz band (THz) are the primary limitations in enabling efficient routing in IBNNs. Our proposed protocol explicitly addresses these challenges and proposes a routing scheme, which enables temperature-aware energy-efficient data transmission to avoid hotspot formation and controlled energy consumption. Furthermore, our proposed temporal correlation based data decision approach allows only those Nano Bio Sensors (NBSs) to transmit the periodic data packets that have updated information for avoiding unnecessary energy consumption and antenna radiation exposure on biological cells. The presented work also considers the instant data retrieval requirement of the healthcare system and introduces an on-demand data retrieval approach that ensures instant transmission of updated information to the healthcare system. The effectiveness of our proposed scheme is evaluated by comparing it with the flooding scheme and thermal-aware routing algorithm (TARA) using the Nano-SIM tool. The results obtained from extensive simulations validate that our proposed protocol achieves 75% - 85 % low temperature rise and improved network lifetime.

INDEX TERMS Energy-efficient, intrabody nanonetworks, molecular absorption noise, routing protocol, terahertz, temperature-aware.

I. INTRODUCTION

Advances in nanotechnology are boosting the development of nanoscale devices [1], which have tremendous potential for enabling cellular monitoring and precision [2], [3]. These nanoscale devices, which consist of data sensing, processing, and computation components, leverage the idea of Intrabody Nanonetworks (IBNNs) [1], [4]. The idea of IBNNs is based on the collaborative effort of a large number of implanted nanoscale devices to empower the emergence of a more sophisticated healthcare monitoring and diagnosis system. Nanoscale devices with their unique features, such as enabling non-invasive cellular level monitoring, early detection of cancerous cells and precision and accuracy in drug delivery and diagnosis are increasing IBNNs potential for a wide range of nanomedicine applications. These nanomedicine applications include in-vivo glucose monitoring system [5], monitoring and detection of cancer biomarkers and human chorionic gonadotrophin [6], [7], which are envisioned to reshape the future of traditional healthcare system.

The emerging scope of IBNNs is leading to a growing interest in addressing the challenges of IBNNs, such as enabling nanoscale communication and the development of

The associate editor coordinating the review of this manuscript and approving it for publication was Oussama Habachi.

novel communication protocols. Among the various methods investigated for enabling nanoscale communication such as molecular communication, nanomechanical communication and acoustic communication [1], Electromagnetic (EM) communication in the Terahertz (THz) band has gained significant attention [8]. The reason behind this rising interest is the development of graphene-based plasmonic nanoantennas that support EM waves propagation in the THz band with the extremely higher bit data rates [4]. Accordingly, the feasibility and scope of EM waves communication in IBNNs is leading to its adaptation for designing EM-based routing schemes [9]–[12]. However, channel modeling in the THz band is regarded as a significant challenge in enabling EM communication in the THz band [13], [14]. EM waves propagation in THz band triggers molecular absorption phenomena, which affects the properties of the propagating medium in terms of attenuation and thermal noise. The issue of thermal noise temperature due to molecular absorption was first highlighted by Jornet and Akyildiz in [14]. Later, other studies [15]–[17] also focused on the molecular absorption noise temperature. In [18], Elayan *et al.* investigated the photothermal effects of molecular absorption in IBNNs. In our previous work [19], we analyzed the thermal effects of nanonodes density on heat generation for the first time. Based on the existing studies [14]–[18], the thermal effects of molecular absorption can cause a rise in the temperature of the body, which can lead to the severe damages to the human body cells, including causing a heat stroke and multiple organ failures.

Thermal un-awareness during routing decisions can also significantly increase the temperature in the biological medium as frequent emission of EM waves for transmitting data increases the biological cells heat exposure time. Furthermore, frequent selection of optimum path (such as shortest route) and unavailability of the next-hop during data transmission is also a major cause of hotspot formation in the biological medium [20]. Thermal-awareness at the network layer has been extensively considered in Wireless Body Area Networks (WBANs) [21]. However, due to different characteristics of IBNNs and WBANs such as energy, transmission range, data rates, storage and computational resources, they are not well suited for unique constraints of IBNNs [22].

The effectiveness of IBNNs routing schemes require a comprehensive understanding of IBNNs thermal challenges along with the in-depth consideration of Nano Bio Sensors (NBSs) limitations in energy, storage, computation and transmission range. The unique feature constraints of these NBSs are illustrated as; NBSs are equipped with severely inadequate energy, with the maximum energy an NBS may harvest, it can transmit only 8 packets of 200 bits during its entire lifetime [9], which significantly reduces the number of messages that can be transmitted by an NBS. In addition to limited energy, the extremely short transmission range of these NBS (i.e., 10 mm) also limits the direct data transmission opportunities. In the context of storage and computational resources, the storage capacity of these NBS does not support maintaining a routing table at the NBS level. Therefore, topology-awareness and selection of an optimum forwarding next-hop are nearly impossible at NBS level [4], [8], [23].

The existing routing schemes in IBNNs [9]–[11], [24] considered only the inadequate energy and storage challenges in designing a routing protocol. To the best of our knowledge a routing protocol that also considers the thermal challenges of a routing protocol has not been proposed. This is the first routing scheme that explicitly considers the energy and thermal challenges of data routing in IBNNs. Our proposed scheme realizes the ultimate objective of saving maximum energy and preventing temperature rise by introducing a temporal correlation based routing scheme. Our proposed temporal correlation based routing scheme increased the transmission of updated information and avoid redundant data transmission for avoiding network resources consumption and heat generation. In addition, we have proposed a novel energy-efficient and thermal-aware forwarded data aggregation approach that facilitates the selection of forwarding hop without storing the topology information at the NBS level. It further aims at the aggregation of multiple forwarded packet transmission into one single copy for transmission to the destination for avoiding hotspot formation and unnecessary energy consumption. The primary contributions of our proposed work are underlined as follows:

1) Our proposed routing protocol is based on temporal correlation to ensure the temperature-aware energy-efficient periodic and on-demand data transmission to the external healthcare system.
2) In our proposed work, we aim to estimate the temperature rise in the biological medium using the Finite-Difference Time-Domain (FDTD) method. Our proposed scheme considers the two primary causes of heat generation in the biological medium, which are described as antenna radiation and molecular absorption noise temperature.
3) We proposed a novel method for data forwarding and aggregation, the intermediate NBSs aggregate the forwarded data for transmitting one single copy to the destination. In addition, our proposed forwarded aggregation methods enable the transmission of critical data with high priority for reducing delay and improving the accuracy of the critical information. We conducted extensive simulation using the Nano-SIM tool to evaluate the performance of our proposed scheme. The obtained results validate that our proposed scheme enables energy-efficient and controlled temperature rise routing in IBNNs as compared to the state-of-the-art schemes.

The rest of the paper is organized as follows: In section II, we discussed the existing scheme in detail. Section III comprehensively demonstrate our proposed temperature-aware energy-efficient routing scheme. Section IV presents performance evaluation, simulation results and discussion of the proposed routing scheme. In Section V, we draw up the conclusion.

II. RELATED WORK

The last decade has witnessed an emerging interest in the development of communication protocols for IBNNs. Research communities have focused their attention on investigating the primary challenges of IBNN (such as channel modeling and designing novel communication protocols) for broadening the scope of IBNNs applications. This section deals with the brief discussion of the thermal challenges associated with EM-based communication in the THz band and the limitations of existing EM-based routing schemes to explore the opportunities and challenges of enabling EM-based routing in IBNNs.

A. THERMAL EFFECTS OF EM-BASED COMMUNICATION IN THE THz BAND

Nanoscale communication using EM waves allows NBSs to communicate in a distributed manner to accomplish diverse responsibilities. However, EM wave propagation in the THz band is severely challenged by the molecular absorption phenomena. Molecular absorption is caused by the movement of the molecules present in the biological medium that affects the medium in terms of attenuation and thermal noise. Molecular absopption noise phenomena can be explained as; the emission of EM waves at specific frequencies in the THz band excites the molecules present in the medium. The excited molecule has an internal vibration, which means the atoms have periodic motion while the movement of the molecule is translational and rotational. Due to this vibration, a part of the energy of the transmitted EM wave is converted into kinetic energy or, from a communication perspective, is simply lost. Subsequently, the internal vibration of the molecules cause the emission of EM radiation at the same frequency as of the propagating incident wave. The amount of radiation that is capable of propagating through the absorbing medium is defined as transmittance, which can be calculated using BeerLamberts law, given in (1):

$$\tau_o(f, d) = e^{-\beta_b d} \tag{1}$$

where f represents the frequency of the EM waves propagating at a distance d, and β_b denotes the molecular absorption coefficients. Jornet *et al.* first determined the value of β_b for gas molecules in [14], which depends on the composition of the medium. Later, Elayan *et al.* [25] followed the same approach for calculating β_b for IBNNs communication using (2):

$$\beta_b = \frac{4\pi(n'')}{\lambda_w} \tag{2}$$

where λ_w represents the effective wavelength defined as $\frac{\lambda}{n'}$, and n', n'' are real and imaginary parts of the tissue's refractive index n. Using the calculated value of the molecular absorption coefficient, the transmittance of the medium is determined as given in [25].

B. EM-BASED ROUTING SCHEME FOR IBNNs

This section briefly discusses the existing EM-based routing schemes to shed light on the limitations of the existing schemes and to emphasize the need for new routing protocols for IBNNs.

The flooding scheme proposed in [26] aimed at conserving energy resources of the IBNN by controlling the direction of the forwarded packets. The selective flooded scheme achieved the objective of energy conservation by avoiding duplicate packets transmission. In [9], a protocol stack was proposed for minimizing energy consumption in IBNNs, the presented greedy scheme selected only a single node for transmitting answer message based on the remaining energy. Selection of a single node for transmitting answer messages supported in reduced energy consumption of the network. Another research effort that attempted to save energy is presented in [10], which employed nanocluster controllers for aggregating data with minimum energy consumption from NBSs. Data transmission to the nanocluster located at the minimum distance reduced data transmission distance and save energy consumption. In [27], the authors examined the energy harvesting options available for NBSs for improved network lifetime. The authors of [11], introduced a fuzzy logic and bio-inspired firefly algorithm based routing scheme for reducing energy consumption during the data reporting process. The optimized selection of NBSs using a bio-inspired firefly algorithm led to an improved network lifetime.

The brief discussion of existing schemes confirm that the primary focus of the state-of-the-art-schemes is on the energy consumption challenges of IBNNs. A routing scheme that also considers the thermal effects of data routing in IBNNs has not been proposed. To the best of our knowledge, this is the first scheme that considers the thermal and energy challenges of IBNNs.

C. EXISTING THERMAL-AWARE ROUTING SCHEME FOR WBANs

The objective of this section is to discuss the existing thermal-aware routing scheme for WBANs to demonstrate the importance of thermal-aware routing scheme. Furthermore, this section also stresses the reasons behind the unadaptability of the existing thermal-aware WBANs schemes for IBNNs. Tang.et.al proposed the Thermal-Aware Routing Algorithm (TARA) in [28]. In TARA, nodes estimate the surrounding temperature by monitoring the activities of their neighboring nodes. Based on the surrounding temperature, the node avoids data transmission in the hotspot area. In another work, Least Temperature Routing (LTR) is proposed [29]. In LTR, the node forwards the packet to the coolest neighbor to avoid hotspot formation while reducing the delay. In another effort to prevent temperature rise, Least Total-Route Temperature (LTRT) routing is performed [29]. LTRT is a hybrid routing scheme that considers the characteristic of the LTR and shortest hop routing algorithm for

TABLE 1. Comparison of our proposed scheme with state-of-the-art-schemes.

Protocol	Network	Energy-efficient	Temperature-aware	Limitations	How temporal correlation method addresses the limitations?
Selective flooding routing scheme [26]	IBNN	Yes	No	Low network lifetime due to a high number of forwarded packets	Reduces the number of packets generated and forwarded to improve network lifetime and avoid temperature rise
Greedy scheme [9]	IBNN	Yes	No	Response message generation by a single node can affect data accuracy; selection of node only on the basis of energy while avoiding other factors such as distance can increase the delay and data forwarding rate	Response messages are generated by enough number of NBSs that ensure high data accuracy while maintaining low energy consumption and temperature rise
An energy conserving routing scheme [10]	IBNN	Yes	No	Nanocontroller aggregate data that increase complexity	Low computational burden on NBSs reduces complexity
Fuzzy logic and bio-inspired firefly algorithm based routing scheme [11]	IBNN	Yes	No	Selection of participating regions and NBSs increases complexity	Simple data transmission decision minimizes complexity
TARA [28]	WBAN	No	Yes	Higher delay and energy consumption due to withdrawal strategy and high packet retransmission rate	Reduced number of packets are generated and forwarded, which minimizes energy consumption and stabilizes temperature rise
LTR [29]	WBAN	No	Yes	Significant increase in power consumption, delay and low data reliability	Minimized overall data traffic helps in maintaining low average delay, temperature rise and improved network lifetime
LTRT [29]	WBAN	No	Yes	Higher packets loss ratio maintains a lower average temperature rise	Low data traffic also increases high packet delivery ratio
HPR [30]	WBAN	No	Yes	Increased request rate interval affects the performance	Even in the high request rate interval, proposed scheme ensures controlled temperature rise and low energy consumption
RAIN [31]	WBAN	No	Yes	Selection of coolest neighbor increases the hop count	NBSs send data to only those next-hop neighbors that have updated information, this approach decreases message overhead and hop-count

selecting the next-hop. In [30], another Hotspot Prevention Scheme (HPR) is introduced that is based on the characteristics of LTR and ALTR. The introduced scheme minimizes the delay while preventing hotspots. In [31], Bag *et al.* proposed a routing algorithm for network of homogeneous and Id-less biomedical sensor nodes (RAIN). RAIN avoids hotspots formation by using a probabilistic approach for next-hop selection. In [32], the authors proposed weighted Based Energy and Temperature aware Routing Protocol (WETRP). WETRP assigns equal weights to residual energy, temperature and link status to distribute data traffic evenly for conserving maximum energy resources, reducing delay and controlling temperature rise.

According to the brief discussion of existing thermal-aware WBAN schemes, we conclude that in WBAN schemes, nodes have enough energy, storage, and computational resources for monitoring the neighboring nodes activities, maintaining a routing tables and accordingly selecting an optimum next-hop. While in IBNNs, NBSs do not have enough resources for storing routing tables and computing next-hop. Therefore, monitoring activities of neighboring NBSs and subsequently selecting the next hop is an over exhausting task for energy constraint NBSs. Moreover, other characteristics of IBNNs (such as transmission range and data rate) also require extensive modifications of existing WBAN schemes before their adaptation for IBNNs. In Table 1, we further highlight the differences between our proposed work and existing schemes to shed more light on the contribution of our work.

III. TEMPORAL CORRELATION BASED TEMPERATURE-AWARE ENERGY-EFFICIENT ROUTING PROTOCOL FOR IBNNs

In this section, we aim to propose temporal correlation based temperature-aware energy-efficient routing scheme, which

explicitly considers the peculiar requirement of IBNNs. The primary objective of our proposed scheme is to prevent temperature rise and reduce energy consumption during transmission of data from NBSs to nanorouter. To address the routing challenges of IBNNs, our proposed routing protocol consists of two different data retrieval mechanisms; named as temperature-aware energy-efficient periodic data retrieval scheme and temperature-aware energy-efficient on-demand data retrieval scheme. Our proposed temperature-aware energy-efficient periodic data retrieval approach aims at minimum consumption of energy resources and controlled heat generation during collection of periodic data from the NBSs. Whereas, the goal of our temperature-aware energy-efficient on-demand data retrieval scheme is to take into account the urgent need for reporting physical parameters in an emergency. Therefore, in the on-demand data retrieval approach, when a nanorouter receives a request message, it selects an optimum number of NBSs for generating response messages. The complete demonstration of proposed NBSs selection mechanism is further discussed in the section III-E. In addition, the Fig. 1 also highlights the working of our proposed scheme.

A. SYSTEM ARCHITECTURE

In this work, we consider a healthcare monitoring system that consists of an IBNN and an external healthcare monitoring system. IBNN encompasses two different kinds of nanoscale devices (i.e., NBSs and nanorouter), which are implanted inside the human body. Implanted NBSs are severely constraint in terms of energy, transmission range, storage and computational resources, whereas nanorouter has more resources than NBSs. Therefore, nanorouters handle more complicated operations, including temperature estimation, data aggregation, and transmission of aggregated information to the external healthcare system using nanointerface. Nanointerface establishes the connection between IBNN and the external healthcare system for remote data transmission via the Internet.

B. NETWORK MODEL, ASSUMPTION AND DEFINITIONS

The considered IBNN is modeled as undirected graph $G = (V, E)$. V is the set of NBSs (NS) and nanorouter(NR) such that $(NS, NR) \in V$. E is the set of edges connecting vertices (i.e. NS and NR). In this work, we assume that NBSs are homogenous, which are deployed using a constant mobility model. Whereas, nanorouter maintains a fixed position.

Definition 1: The temporal correlation proportion is based on the reading reported by the NBS (NS_i) during last periodic data interval denoted as $PR_{tran}^{(t(i-1))}$ and the value observed by the NBS (NS_i) for the current periodic interval expressed as $CR_{obs}^{(t(i))}$. Temporal correlation proportion value determine the correlation between the current observed and previous transmitted reading using (3).

$$C(proportion) = \left(\frac{|\ CR_{obs}^{(t(i))} - PR_{tran}^{(t(i-1))}\ |}{CR_{obs}^{(t(i))}}\right) \times 100 \qquad (3)$$

where $CR_{obs}^{(t(i))}$ and $PR_{tran}^{(t(i-1))}$ denotes the value observed in the current periodic interval and the value transmitted in the previous periodic interval, respectively.

Definition 2: A location μ in the event area A is designated as a hotspot, if location μ has a temperature rise greater than the specified threshold (i.e, the normal temperature of the body).

Nanorouter estimates the change in temperature by monitoring the activities of the NBSs in location μ. Let us consider that location μ is covered by n number of NBSs. The NBSs located in the location μ can be same and different at different time instances (i.e. due to movement of NBSs). NBSs positioned at location μ at various time intervals can be expressed as $\{(\mu_{I(i)}, \{s_i, s_k, .., s_n\}), (\mu_{Ii+1}, \{s_j, s_k, .., s_n\}), \ldots.(\mu_\tau, \{s_x, s_y, .., s_w\})\}$. After each request rate interval, nanorouter calculate the temperature rise in location μ. The rise in temperature is a function of power radiated by n number of NBSs and molecular absorption noise due to heat absorption in the biological medium.

C. TOTAL TEMPERATURE RISE ESTIMATION

In this section, we aim to provide a detailed explanation of the temperature rise estimation process. In our proposed protocol, nanorouter calculates the increase in the temperature by considering the two main contributors of heat generation in the biological medium (i.e., antenna radiation and molecular absorption noise temperature). NBSs radiate EM waves into the biological medium for transmitting data, the radiated energy is absorbed by the surrounding biological cells that emit this absorbed energy as heat into their surroundings. Consequently, emitted energy leads to increased molecular absorption noise temperature, which increases the observed temperature of the biological medium. Temperature rise at location μ is calculated using diffusive heat equation [32], expressed in (4). We have assumed the biological tissues to be homogeneous without any sharp edges.

$$K\nabla^2 T + \Delta T_{mol} + \Delta T_{rad} + Q_{heat} = \rho C_p \frac{\partial T}{\partial t} \qquad (4)$$

where the mass density and specific heat capacity of the heated particle are denoted using ρ and C_p, respectively. The rate of change of temperature is expressed as $\frac{\partial T}{\partial t}$, K denotes the thermal conductivity and ΔT_{mol} shows the change in temperature caused by molecular absorption noise temperature. ΔT_{rad} represents the temperature increased due to antenna radiations and Q_{heat} is the rate of generated heat energy per unit volume. Q_{heat} can also be described as the energy source formed due to EM absorption in the particle [33], [34].

1) ANTENNA RADIATIONS

NBSs equipped with point dipole antenna are the primary source of heat generation in the biological medium. The length of point dipole antenna is denoted using l, and the dipole movement $I_o l$ is set to 1mA. The electric field intensity of a point dipole antenna is determined using the geometry of the radiating antenna and its current distribution.

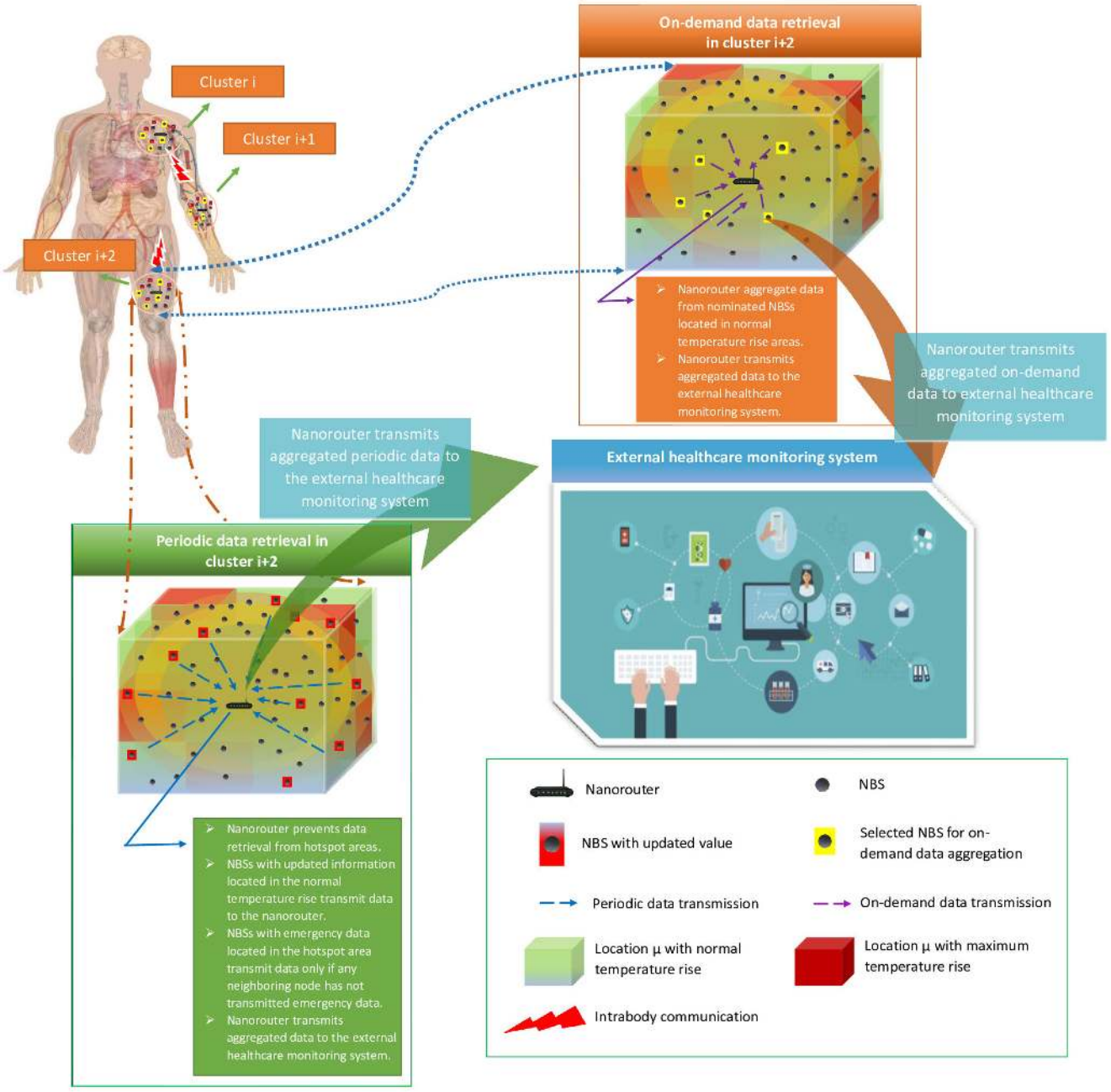

FIGURE 1. **Illustration of proposed protocol model: Before periodic data retrieval nanorouter estimates increase in the temperature and avoid data collection from the hotspot areas. Those NBSs that are located in the normal temperature rise area transmit the periodic data based on temporal correlation decision. Whereas for on-demand data retrieval, nanorouter nominates those NBSs that are located in the normal temperature rise area and have maximum selection score. Subsequently, nanorouter transmits the aggregated data to the external healthcare system.**

A half-wavelength dipole antenna experiences maximum intensity at ($\theta = \frac{\pi}{2}$) [18], which can be expressed using (5):

$$|E_\theta(r)|_{\theta=\frac{\pi}{2}} = \frac{120}{r}\sqrt{\frac{P_o}{2R_o}} \tag{5}$$

where the angle between the antenna axis and the vector to the observation point is denoted as θ, the distance to the antenna, and the average power radiated by the antenna is expressed using d and P_o. The average radiated power P_o can be calculated using (6):

$$P_o = \frac{1}{2}R_o I_o^2 \tag{6}$$

where R_o denotes the radiation resistance of the antenna, determined using (7):

$$R_o = 20\pi^2(\frac{l}{\lambda})^2 \tag{7}$$

where l is the length of antenna, the total heat generated in a location μ is determined by combining the power radiated by

n number of radiating antenna that emit EM waves, as given in (8):

$$\Delta T_{rad} = \sum_{n=1}^{N} Power_n^{rad} \tag{8}$$

where the coefficient $Power_n^{rad}$ represents the power radiated by N antennas.

2) MOLECULAR ABSORPTION NOISE TEMPERATURE

The energy absorbed by the surrounding cells due to exposure of EM waves leads to an increase in molecular absorption noise temperature. The rise in temperature is determined using the heat model developed in [18]. The heat generated from the $N_{par} - 1$ particles located at the nearest distance d_n from the heat emitting source d_s (i.e. antenna) can be rewritten as [18], using (9):

$$\Delta T_p = \sum_{n=0;m\neq s}^{N_{par}} \frac{Q_{par}}{4\pi \hat{K}} \frac{1}{\mid d_s - d_n \mid} \tag{9}$$

where $\hat{K} = \frac{k+k_o}{2}$, and Q_{par} is the heat produced by the N_{par} that absorbed the heat and became the heat sources. The overall change in temperature is estimated by determining the heat produced in the medium. According to the law of conservation of energy, the heat generated (Q_{in}) is equivalent to heat dissipated (Q_{out}), hence change in temperature can be calculated using (10):

$$\Delta T = \frac{Q_{in}}{Q_{out}} \tag{10}$$

where Q_{in} and Q_{out} shows heat generated and heat dissipated by the heat particle, given in (11) and (13):

$$Q_{In} = \sigma_{abs} I_o V_{NP} \tag{11}$$

where I_o is the light intensity and σ_{abs} is the absorption cross section calculated as (12):

$$\sigma_{abs} = (\alpha) * (\beta_{abs}) \tag{12}$$

where α is the density of the heat particles N_o in volume V_o and β_b is the molecular absorption coefficient defined in (1). Heat dissipated Q_{out} can be calculated as (13):

$$Q_{out} = 4\pi r \hat{K}; \tag{13}$$

Now we estimate the temperature rise in the location μ can be following the similar approach used in [18], [33]. We considered the surface area of the location μ is a small cuboid of volume V, where identical heat particles N_{par} are extended over the cuboid, the molecular absorption noise temperature can be calculated using (14):

$$\Delta T_{mol} = \int_{z_{min}}^{z_{max}} \int_{y_{min}}^{y_{max}} \int_{x_{min}}^{x_{max}} \frac{Q_{hp}}{4\pi \hat{K}} \, dx \, dy \, dz \tag{14}$$

where Q_{hp} is the heat produced by identical particles. Further, expression of ΔT_p varies according to the typical array geometry and various illumination conditions [18], [33].

3) TEMPERATURE RISE CALCULATION USING FDTD

The total temperature rise is estimated using FDTD approach. FDTD is an EM modeling technique that discretizes the differential form of time and space. Due to the low complexity of FDTD in terms of time and memory, it is suitable for measuring heat gain [28]. Now we modify the bioheat equation given in (4) for calculating temperature rise in location μ using FDTD technique. The location μ is presented using three coordinates (x, y, z). The new modified heat equation for overall temperature rise is expressed in (15):

$$\begin{aligned} T^{t+1}(x,y,z) = &\left[1 - \frac{6K\delta t}{\rho C_p \delta^2}\right] T^t(x,y,z) + \left[T^t(x+1,y,z)\right. \\ &+ T^t(x-1,y,z) + T^t(x,y+1,z) \\ &+ T^t(x,y-1,z) + + T^t(x,y,z+1) \\ &\left. + T^t(x,y,z-1)\right] \frac{K\delta t}{\rho C_p \delta^2} + \frac{\delta t(\Delta T_{mol})}{\rho C_p} + \frac{\delta_t T_{rad}}{\rho C_p} \end{aligned} \tag{15}$$

where T^{t+1} is the temperature of the location μ (x, y, z) at time $t+1$, δ_t and δ are discretized time step and the discretized space step respectively. From this equation, we can find the temperature of the location μ (x, y, z) at time $t + 1$, which is a function of the temperature at location μ (x, y, z) at time t, as well as a function of the temperature of surrounding locations $(x + 1, y, z)$, $(x - 1, y, z)$, $(x, y + 1, z)$, $(x, y - 1, z + 1)$, $(x, y, z + 1)$, and $(x, y, z - 1)$ at time i.

D. TEMPERATURE-AWARE ENERGY-EFFICIENT PERIODIC DATA TRANSMISSION

The implanted NBSs are responsible for generating periodic data packets at specified time intervals that consume significant energy resources of NBSs and require frequent emission of EM waves in the medium. To enable energy-efficient periodic data transmission with controlled temperature rise, we have proposed a temporal correlation based routing scheme. The purpose of employing temporal correlation is the nature of the continuous glucose monitoring applications, which exhibits a significant temporal correlation among the consecutive detected reading. In IBNNs, the transmission of temporally correlated information results in the collection of similar information at the expense of energy resources and increased heat generation. Therefore, we have proposed a temporal correlation based periodic data transmission mechanism, which ensures that NBSs do not frequently radiate EM waves for transmission of similar information. Since NBSs consume maximum energy during data communication and high data communication rate affects the networks in terms of increased antenna radiation exposure and energy consumption. Therefore, evading redundant data transmission support in achieving steady temperature rise in the biological medium and reduced energy consumption.

1) HOTSPOT IDENTIFICATION

Due to the limited resources of NBSs, they are unable to efficiently estimate the change in their surrounding

temperature. Therefore, nanorouters are responsible for enabling temperature-aware parodic data transmission. Nanorouter monitors the change in temperature and prevents parodic data retrieval from the hotspot areas. Nanorouter identifies hotspot areas by estimating temperature rise using (15) after every parodic data transmission interval and broadcast information about the hotspot areas. Any location μ in the coverage area that has estimated temperature rise above the allowed temperature threshold is excluded from the generation of periodic data packets. The temperature threshold is set according to the average temperature of the body. The restriction of parodic data transmission avoids any further antenna exposure on biological cells in the hotspot areas and provide enough time to the heated region to stabilize its temperature.

2) PERIODIC DATA RETRIEVAL FROM NORMAL TEMPERATURE RISE AREAS

NBSs that are located in the areas with normal temperature rise are allowed to generate parodic data packets. The complete mechanism of temporal correlation based data transmission decision and data transmission process is elaborated in this section.

a: TEMPORAL CORRELATION BASED DATA TRANSMISSION DECISION

To eliminate similar data transmission, NBSs decide about the data transmission by determining the temporal correlation proportion using (3). Based on temporal correlation proportion, we have constructed the following binary hypothesis given in (16):

$$\begin{cases} R(T) : C(Propation) > \phi \\ R(S) : C(Propation) \leq \phi \end{cases} \tag{16}$$

where ϕ is the Temporal Coherency Threshold (TCT). If the value of the temporal correlation proportion is higher than the TCT, then the data transmission decision is positive, which means that NBS has updated detected value that needs to be transmitted. Whereas, if $R(T)$ is 1, then the observed reading is similar, and the detected value is suppressed.

b: DATA TRANSMISSION

Once data transmission decision is made, NBSs with the positive updated information (active NBSs) transmit data to the nanorouter via a single-hop or multi-hop method. Active NBSs broadcast announcement messages to notify neighboring NBSs about their transmission. The announcement message contains the information about the NBS ID and its respective layer based on the closeness degree of the NBS (i.e., the distance between a nanorouter and the NBS).

Definition 3: NBSs located in the transmission radius of the nanorouter are associated to different layers based on the closeness degree, the different layers are expressed as; $\{\alpha_r, \alpha_{r-1}, \alpha_{r-2} \ldots . \alpha_{r-n}\}$. *The number of layers depends on the transmission radius of the nanorouter and transmission radius of the NBSs determined as* $n = (Tran.radiusofnanorouter/Tran.radiusofNBS)$. *The width of each layer corresponds to the transmission radius of the NBS to enable direct data transmission from the lower layer to the intermediate higher layer. The highest layer is expressed as the* α_r, *which is the nearest layer from the nanorouter.*

Algorithm 1 Temperature-Aware Energy-Efficient Periodic Data Retrieval From Normal Temperature Rise Areas

1: **Input:**
2: NS = List of NBSs
3: **Action:**
4: **For** each NS_i do
5: $PR_{tran}^{(t(i-1))}$ = Previously transmitted reading
6: $CR_{obs}^{(t(i))}$ = Current observed reading
7: **END For**
8: **For** each NS_i do
9: Determine temporal correlation proportion using (3)
10: **If** temporal correlation proportion $> \phi$ (TCT) **Then**
11: Transmit the detected reading
12: **Else**
13: Suppress the detected reading
14: **END For**

The Broadcast of announcement messages provides an opportunity to the topology un-aware NBSs about the possibility of data transmission through an optimum forwarding next-hop. NBSs select only those NBSs for forwarding periodic data that have broadcast the announcement messages. The twofold objective of our proposed forwarded data aggregation scheme is elaborated as; first, excluding the involvement of inactive NBSs in data forwarding for saving their energy that will be consumed in data forwarding. Second, avoiding transmission of multiple forwarded packets by combining the packets at the intermediate forwarding NBSs and transmitting one single copy to the destination for conserving energy and preventing heat generation.

3) PERIODIC DATA RECEIVAL FROM HOTSPOT AREAS

Based on the announcement of nanorouter about hotspot areas, NBSs located in the hotspot areas cannot transmit the periodic data even if they have updated information. NBSs only generate periodic messages if they have detected high priority information that cannot be suppressed. The NBSs that transmit the high priority information is overheard by the NBSs, which are located in the close vicinity. Correspondingly, other NBSs with the high priority information stop their transmission with the objective of saving biological tissues from overexposure of EM waves. The data transmission mechanism from the hotpot area is further demonstrated in Algorithm 2.

4) PERIODIC DATA AGGREGATION AT THE INTERMEDIATE NBSs

After receiving data from the lower layer, the intermediate forwarding NBSs perform low complexity operations to

Algorithm 2 Temperature-Aware Energy-Efficient Periodic Data Retrieval From Hotspot Areas

Input:
NS = List of NBSs
Action:
For each NS_i do
$PR_{tran}^{t(i-1)}$) = Previously transmitted reading
$CR_{obs}^{(t(i))}$ = Current observed reading
$Data_{type}$ = {Emergency,Regular}
End For
For each NS_i do
If ($Data_{type}$ = Emergency && neighboring NBSs have not transmitted the packet) **Then**
Transmit the packet
Else If ($Data_{type}$ = Regular) **Then**
Do not transmit the packet and store in the buffer
End For

combine the data packets for transmitting a single data copy to the destination. Our proposed forwarded data aggregation method combines the data based on the priority of the transmitted packet and forwarding similarity threshold.

Definition 4: The periodic reading received at the intermediate NBS for the interval ($t(i)$) *denoted as* ($PRR_{t(i)}$) *and the periodic reading detected for the interval* ($t(i)$) *at the intermediate NBS denoted as* ($PRD_{t(i)}$) *are correlated if forwarding correlation proportion is less than or equal to forwarding similarity threshold, forwarded data correlation can be calculated as* (17)*:*

$$FDC(proportion) = \left(\frac{|\ PRD_{t(i)} - PRR_{t(i)}\ |}{PRD_{t(i)}} \times 100\right) \leq \sigma \quad (17)$$

where $PRD_{t(i)}$ *and* $PRR_{t(i)}$ *denotes the periodic reading detected and received at the intermediate NBS, respectively. While* σ *represents the forwarding similarity threshold. In this work, we consider the value of* σ *to be 15% that can be changed according to a specific application.*

The aggregation of the data is performed according to the forwarding similarity threshold and data priority level of the source and intermediate NBS.

Definition 5: The priority of the data is set according to the characteristics of the application. In our proposed work, we have defined the data criticality level according to hypoglycemia condition for the low and high level of glucose given in [35]. For a low glucose level, the critical levels are defined as low glucose level 1 (LGL1) and low glucose level 2 (LGL2). The glucose range of LSL1 is given as ($70\ mg/dL < Glucose \geq 54 mg/dL$)*, which is categorized as low-level hypoglycemia alert that requires instant monitoring. In LSL2, the glucose reading of* $< 54\ mg/dL$ *signifies very low-level hypoglycemia and requires immediate action. While the priority of high glucose level is classified as high glucose level 1 (HGL1) and high glucose level 2 (HGL2). HGL1 has reading* ($250\ mg/dL \leq Glucose > 180\ mg/dL$)*, considered as the elevated high glucose level and require immediate monitoring. Whereas glucose value of greater than* $250\ mg/dL$ *is indicated as the HGL2 necessitating immediate action.*

The mechanism of data aggregation based on data priority level (i.e. LGL1, LGL2, LGL3 and LGL4) and forwarding similarity threshold is demonstrated below in detail:

1) Intermediate NBS and source NBS both have data priority of the same level: The Intermediate NBS calculates forwarding correlation proportion using (17) and compares it with forwarding similarity threshold. In this case, let intermediate NBS A and source NBS B both has same priority level and $FDC(proporation) < \sigma$, then it is comprehended that NBS A has reading that is similar to the reading received from NBS B. Thus, average operation is performed to combine the readings of NBS A and NBS B. Aggregation from multiple sources that have transmitted almost the similar readings is performed using (18):

$$HPR_{agg} = \frac{PRD_{int} + \sum_{k=0}^{k=n}(PRR_k)}{k+1} \quad (18)$$

where PRD_{int} denotes observed reading at intermediate NBS and (PRR_k) shows the number of similar readings received at intermediate NBS from multiple NBS.

2) Intermediate and source NBS have the value of different data priority levels: Let us assume intermediate NBS A has a value of data priority level (LGL1 or low priority level) and source NBS B has a value of data priority from any other data priority level (i.e., LGL2, HGL1 or HGL2). Intermediate NBS compares the calculated forwarded data correlation with the forwarding similarity threshold and checks the priority of the received packet. If the $FDC(proporation) \nleq \sigma$ and data priority of the received packet are high, then intermediate NBS does not combine it with any other reading unless the intermediate NBS has already received readings from the same priority level.

3) Intermediate NBS has a value of data priority level (LGL1, LG2, HGL1 or HGL2) and the source NBS has low priority data: The intermediate NBS compares the estimated forwarded data correlation with forwarding similarity threshold. If forwarding similarity threshold is greater than the similarity (i.e. $FDC(proporation) \nleq \sigma$) and received data has low priority data. Then intermediate NBS considers this information as a low weighted data and adds it to the other similar low priority readings, as given in equation (19):

$$LPR_{agg} = \frac{\sum_{k=0}^{k=n}(PRR_k^{LPL})}{k} \quad (19)$$

where PRR_k^{LPL} denote the low periodic reading received. After intermediate NBS has received all the readings, intermediate NBS assign low weightage (ω_2) to low priority readings given in Equation (19) and high weightage to high priority readings calculated in

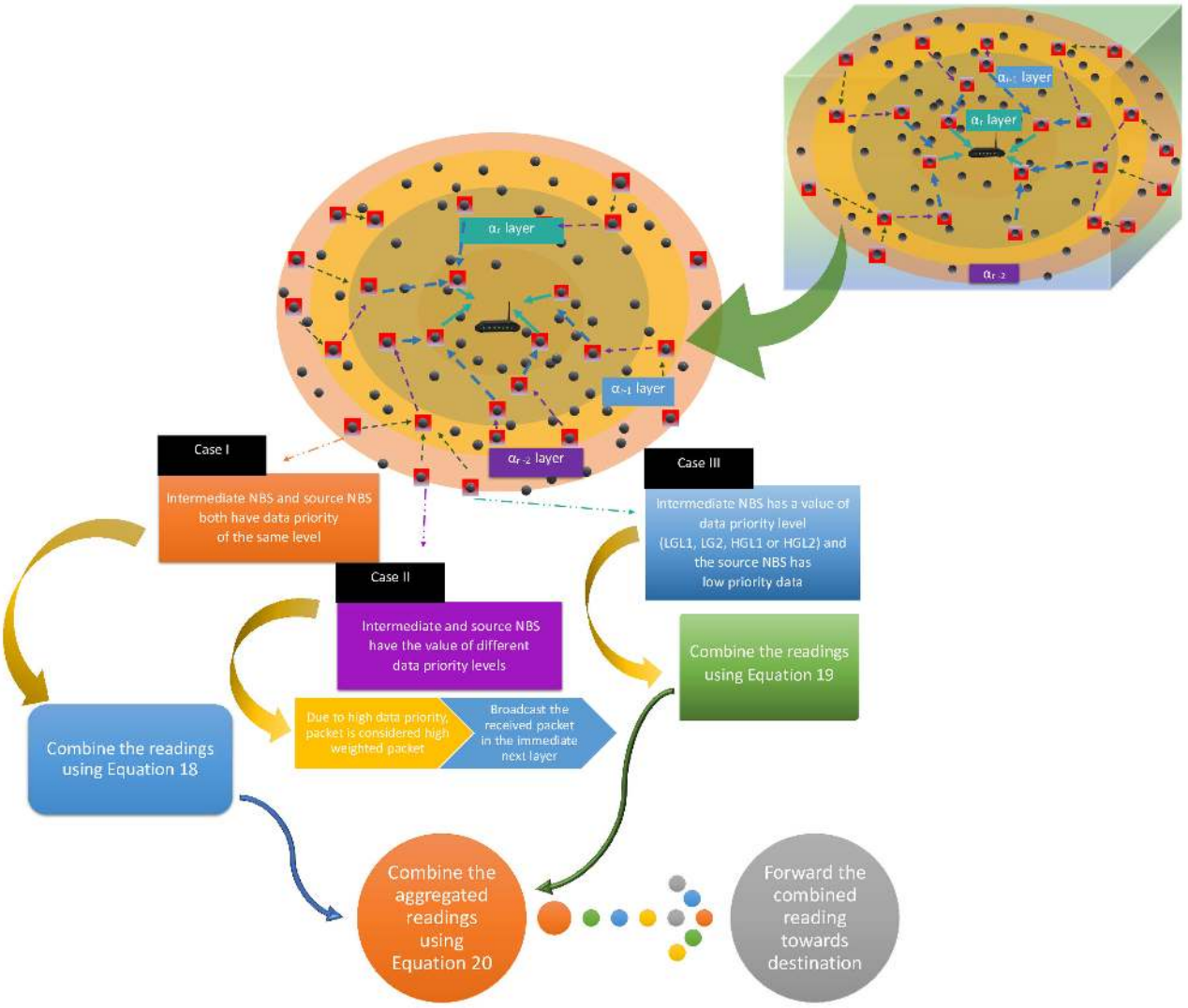

FIGURE 2. Periodic data aggregation at the intermediate NBSs: Intermediate NBSs combine the received forwarded packets using proposed forwarded aggregation mechanisms and forward one single copy towards the destination.

equation (18), such that the assigned weights $\omega_1 + \omega_2$ are equal to 1. Finally the accumulated reading is calculated using (20).

$$DR_{agg} = (\omega_1) \times (LPR_{agg}) + (1 - \omega_2) \times (LPR_{agg}) \quad (20)$$

E. TEMPERATURE-AWARE ENERGY-EFFICIENT ON-DEMAND DATA RETRIEVAL

Diagnosis and treatment of physiological parameters also demand instantaneous collection of detected readings. Therefore, we have introduced an on-demand data retrieval mechanism; the objective of our proposed scheme is to enable instant transmission of data to the healthcare system when a request is made. The on-demand data transmission approach outlines our proposed scheme more proactive about the patients health condition. To realize the goal of our proposed approach, nanorouter handles the immediate requirement of diverse healthcare parameters by selecting the optimum NBSs for generating on-demand answer packets from those regions that are not experiencing temperature rise. The proposed selection standard is regulated by nanorouter that nominates NBSs based on their most recent transmission interval, estimated residual energy and distance from nanorouter. The reason behind our unique selection parameter of the most recent transmission interval is to increase the probability of receiving updated information as those NBSs that have recently transmitted updated information are more likely to have meaningful information. While the other selection parameter (i.e., residual energy and distance) strengths selections of those NBSs whose participation will not cause the death of the network and reduces multi-hop transmission. The mathematical expression for the aforementioned selection is given in (21):

$$Selection_{points} = \begin{cases} \dfrac{MRTI_{NS} + E_R}{D_{NS \to NR}} & if\, E_R > E^t \\ 0 & \text{otherwise} \end{cases} \quad (21)$$

where $MRTI_{NS}$, E_R, and $D_{NS\rightarrow NR}$ represents the most recent transmission interval of the NBS, residual energy, and distance of NBS from nanorouter, respectively. The nanorouter nominates those NBSs for transmitting answer messages that have a maximum $Selection_{points}$.

F. ENERGY CONSUMPTION ANALYSIS

The objective of presented section is to perform a detailed energy consumption analysis of IBNN by considering the number of messages transmitted and received by nanotransceivers using the TS-OOK modulation scheme at the physical layer [36]. Based on the TS-OOK modulation scheme, the energy expended during transmission of a pulse is 1 pJ (i.e., $E_{tx} = 1\,pJ$), whereas the energy consumed during the pulse reception is 0.1 pJ (i.e., $E_{rx} = 1\,pJ$). Accordingly, (22) and (23) provide the amount of energy consumed during transmission and reception of x number of bits.

$$E_{tx}(x) = x \times \gamma \times E_{tx}^{pulse} \tag{22}$$

$$E_{rx}(x) = 0.1 \times x \times E_{rx}^{pulse} \tag{23}$$

where γ represents the transmission probability of symbol 1 in the x streams of bits, and its weight is generally set to 0.5 as 0 and 1 both have the same probability of occurrence. Whereas, during the reception process, the entire stream of bits is considered.

Accordingly, the amount of energy consumed after *rth* periodic interval is expressed as (24):

$$E_{con.}^{rth} = NT(M_{AM}) \times E_{tx} + NT(M_{AN}) \times E_{tx} + NR(M_{AM}) \times E_{rx} + NR(M_{AN}) \times E_{rx} + NR(M_{RM}) \times E_{rx} + E_H \tag{24}$$

where $NT(M_{AM})$ and $NT(M_{AN})$ shows the total number of transmitted answer message and announcement messages. Whereas, $NR(M_{AM})$, $NR(M_{AN})$ and $NR(M_{RM})$ denote total number or received answer messages, announcement messages, and request messages respectively. The amount of energy harvested during the periodic time interval (t) is expressed using E_H.

In the context of the energy harvesting mechanism, the technical limitations of nanonetworks do not support conventional energy harvesting mechanisms such as solar energy, wind power, and underwater turbulence. To address these energy harvesting challenge, novel schemes are proposed for recharging nanoscale devices. One of the prominent techniques of energy harvesting is the introduction of a piezoelectric nanogenerator [37]. The piezoelectric nanogenerator is composed of an array of ZnO nanowires, a reflecting circuit, and an ultra nanocapacitor. The nanowires compression produces an electric current between the ends of nanowires that recharge the ultra nanocapacitor. The mechanical vibration methods such as air conditioning and heartbeat provide the compressed release cycle. The frequency of the compressed release cycles f_c provides the time for recharging the ultra nanocapacitor. Based on the energy harvesting model, the voltage of the charging nanocapacitor after β compressed cycles can be rewritten as [37], using (25):

$$V_{cp}(\beta_{cycles}) = V_g \times (1 - e^{-\frac{\beta_{cycles}\Delta Q}{V_g C_{cp}}}) \tag{25}$$

where C_{cp} denotes the total capacitance of the ultra nanocapacitor, V_g shows the generator voltage and ΔQ represents the harvested charge per cycle. The typical values of these quantities C_{cp}, ΔQ and V_g are 9 cF, 6 pc and 0.42 V respectively. According to [37], after β_{cycles} the energy E_{cp} stored in ultra-nanocapacitor is given using (26):

$$E_{cp}(\alpha) = \frac{1}{2} C_{cp}(V_g(\beta_{cycles})^2) \tag{26}$$

where C_{cp} represents the capacitance of ultra-nanocapacitor, V_g corresponds to the voltage of the generator and β_{cycles} demonstrates the number of cycles necessary to reach the energy level given by (27):

$$\beta_{cycles}(E) = \left\lceil \frac{-V_g C_{cp}}{\Delta Q} ln\left(1 - \sqrt{\frac{2E}{C_{cap} V_g^2}}\right) \right\rceil \tag{27}$$

where V_g is the generator voltage, C_{cp} is the capacitance of ultra-nanocapacitor and ΔQ represents the harvested charge per cycle. Subsequently, the amount of energy harvested during periodic time interval (t) is obtained by determining the number of cycles β required for charging the ultra-nanocapacitor, as expressed in (28):

$$E_H^t = E_{cp}(cycles_\beta + cycles_{(t)}) \tag{28}$$

where $cycles_\beta$ correspond to number of cycles given in (27) and $cycles_t$ represents the number of cycles during the periodic time interval (t).

In the view of the amount of energy harvested and consumed in packet transmission and reception process, the remaining energy of the network is obtained using (29):

$$RE_{NW} = E_o - E_{con.}^t \tag{29}$$

where E_o denote the initial energy of the network and $E_{con.}^t$ represents the amount of energy consumed till the periodic time interval (t).

IV. PERFORMANCE EVALUATION

This section evaluates the proposed routing scheme in IBNNs to highlight the practical utility of the proposed protocol for healthcare applications. To shed light on the efficacy of the proposed scheme, we have performed an extensive comparison with the flooding scheme and TARA. The flooding scheme is considered as the benchmark scheme for comparing new routing schemes for IBNNs. In the flooding scheme, the direction of the forwarded packets is controlled to save energy and bandwidth [26]. Whereas, In TARA each node monitors the activities of its neighboring nodes for preventing forwarding data in a hotspot area [28]. The reason behind using TARA is the unavailability of a thermal-aware scheme for IBNNs. Furthermore, the detailed comparison

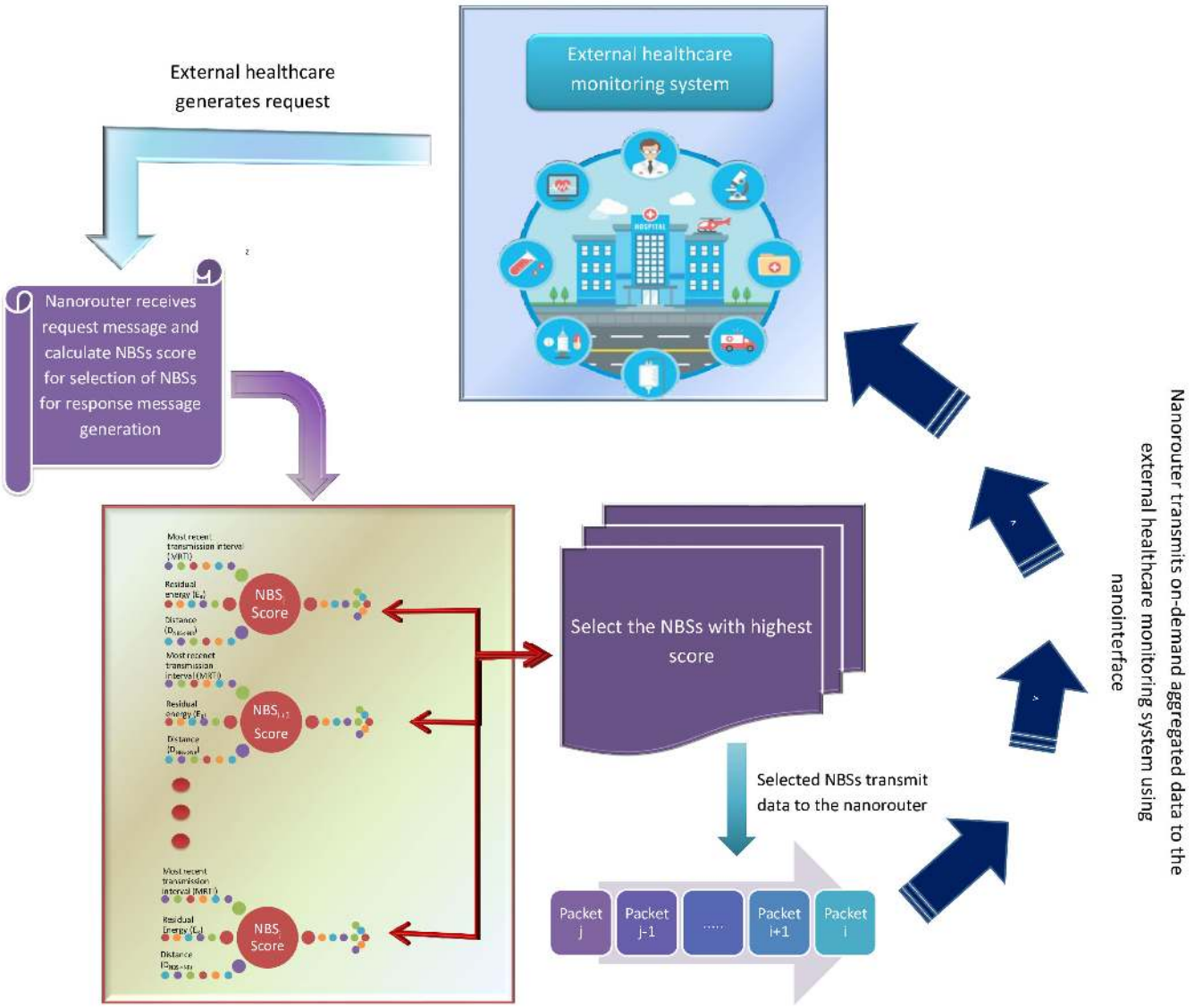

FIGURE 3. On-demand data retrieval process: In response to the received request message, nanoroute calculate NBSs $selction_{points}$ to nominate NBSs for data transmission. NBSs with the maximum $selction_{points}$ transmit data to the nanorouter.

with TARA also underlined the significant energy consumption and delay issues of TARA regarding its adaption in IBNNs.

A. NANO-SIM SIMULATIONS

We have performed detailed simulations using the Nano-Sim tool. The Nano-Sim tool is an emerging tool integrated into NS-3 for evaluating the performance of EM-based communication schemes in the THz band [26]. We consider an IBNN, which is expended on a radius of 10 mm with a varying number of NBSs (i.e., 100 and 150) and one nanorouter. The implanted NBSs are moving in the network area using a constant mobility model, whereas, nanoroute maintains a fixed position at the center of the network during the entire simulation time. The moving NBSs are equipped with a sensing unit for monitoring the physiological parameters. NBSs transmit detected physiological readings to the nanorouter at the periodic intervals and on the demand of the external healthcare system. At the physical layer, we have adapted the same settings as given in [36]. The size of answer messages is set to 176 bits. Whereas, the size of the request message and announcement message flowing in the network is set to 36 bits. For providing a fair comparison, we have used the same simulation parameters for all the schemes. Furthermore, table 2 summarizes the tissues' properties for IBNNs along with the simulation parameters. We consider the same properties of the tissues as adapted in [18] for photothermal modeling of IBNNs.

B. PERFORMANCE METRICS

We use the following metrics to evaluate the performance of our proposed scheme.

TABLE 2. The values of the simulation parameters selected for the simulations.

Parameters	Values	Parameters	Values
Number of NBSs	100 and 150	Transmission range of NBSs (mm)	10
Initial energy of NBSs (pJ)	800	Time to Live (TTL) value	100
TCT	(10%,15%,20%,25%,30%)	Temperature threshold (K)	310.15
Red blood cell thermal conductivity (k_p)	$0.52W/m/^oC$	Pulse energy (pJ)	100
Blood plasma thermal conductivity (k_o)	$0.58W/m/^oC$	Pulse duration (fs)	100
Red blood cell density	$1025kg/m^3$	Pulse interval time (ps)	10
Red blood cell specific heat capacity (C_p)	$3617j/kg/^oC$	Total iteration	10
Red blood cell radius (a)	4×10^{-6}	Simulation duration (seconds)	3

- Average temperature rise: Average temperature rise represents the average increase in the temperature observed in the network.
- Average remaining energy: This represents the average energy left in the network.
- Alive NBSs: It shows the number of alive NBSs in the network.
- Number of notifications: It corresponds to the total number of readings reported by the NBSs.
- Average end-to-end delay: It expresses the average end-to-end delay experienced by a packet.
- Packet delivery ratio: It represents the total number of packets transmitted to the total number of packets received.

C. SIMULATION RESULTS

This section provides a comprehensive discussion of the obtained results to highlight the potential of the proposed scheme for enabling continuous healthcare monitoring. The presented results have 95% confidence interval computed after 10 iterations to reduce statistical fluctuations impact.

1) AVERAGE TEMPERATURE RISE COMPARISON OF OUR PROPOSED SCHEME WITH THE DENSITY OF 100 NBSs AND INCREASING TCT OVER TIME

Fig. 4 demonstrates that increased traffic rate also increases the heat generation. Therefore, from Fig. (4a,4b), we can observe that in WFCS, the increase in the temperature is 40% more than our proposed scheme. Our proposed scheme and WFCS, both experienced the maximum temperature rise at 10% TCT due to high packet generation rate. However, our proposed scheme still observed a low temperature rise due to our efficient forwarded data aggregation scheme, which prevents the biological medium from overheating. Whereas, the flooding scheme experienced the maximum temperature rise for all the TCT values (i.e., 10%, 15%, 20%, 25% and 30%), due to thermal-unawareness during routing decisions. While TARA experiences more temperature rises due to higher packet generation and packet forwarding rate, which ultimately increases the temperature. Fig. 4a depicts that once the network is dead the flooding scheme and TARA experience no further change in the temperature. To shed more light on the contribution of our proposed scheme on low average temperature rise, we have also compared the average temperature rise observed at the end of simulations (see Fig. 4c). Fig. 4c, demonstrate that our proposed scheme realizes the objective of controlled temperature rise by enabling temperature-aware routing and controlled traffic flow.

2) AVERAGE TEMPERATURE RISE COMPARISON OF OUR PROPOSED SCHEME WITH THE DENSITY OF 150 NBSs AND INCREASING TCT OVER TIME

Fig. (5a,5b) shows that for increasing densities of NBSs, our proposed temperature-aware routing scheme maintains a steady temperature rise whereas WFCS results in a high temperature rise due to forwarding of all packets without any aggregation at the intermediate NBS. The flooding scheme and TARA experience more rise in temperature than our proposed scheme due to the high rate of traffic generation and data forwarding. In Fig. 5c, the average temperature rise at the end of simulations is presented to highlight the impact of our proposed scheme further. From Fig. 5, we can observe that our proposed scheme achieves the objective of hotspot prevention and maintains the lowest average temperature rise.

3) AVERAGE REMAINING ENERGY COMPARISON OF OUR PROPOSED SCHEME WITH THE DENSITY OF 100 NBSs AND INCREASING TCT OVER TIME

Fig. 6a depicts that the increasing value of TCT leads to lower consumption of energy resources. In WFCS, the maximum energy is consumed for 10% TCT. Whereas, for our proposed scheme even at 10% TCT energy consumption is lower than WFCS for all the TCT values (i.e, 10%, 15%, 20%, 25% and 30%). When TCT is set to 30%, our proposed scheme experienced the lowest amount of energy consumption due to suppression of the maximum number of notifications.

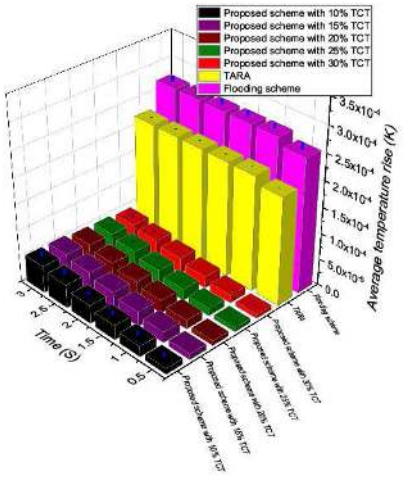

(a) Comparison of average temperature rise observed in our proposed scheme with the flooding scheme and TARA.

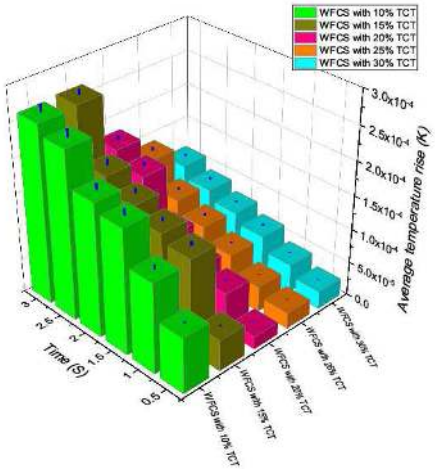

(b) Average temperature rise observed in WFCS.

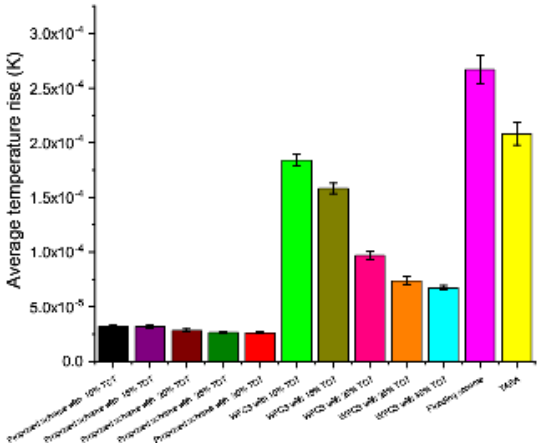

(c) Average temperature rise comparison at the end of simulations.

FIGURE 4. Average temperature rise comparison of our proposed scheme with WFCS, the flooding scheme, and TARA with the density of 100 NBSs and increasing TCT over time.

Fig. 6b represents the comparison of our proposed scheme with the flooding scheme and TARA to shed more light on the impact of our proposed scheme on remaining energy. From Fig. 6b, it is evident that our proposed scheme improves 70% to 80% better residual energy as compared to both TARA and the flooding scheme. The reason behind improved remaining energy is our proposed temporal correlation based data transmission decision that suppresses the redundant data transmission and enables transmission of updated information, which ultimately results in better remaining energy.

4) AVERAGE REMAINING ENERGY COMPARISON OF OUR PROPOSED SCHEME WITH THE DENSITY OF 150 NBSs AND INCREASING TCT OVER TIME

From Fig. 7, it is evident that the increased NBSs density improves the residual energy of the network. Our proposed scheme achieves the maximum remaining energy for all the TCT values (i.e, 10%, 15%, 20%, 25% and 30%). Whereas in WFCS, energy delation is more rapid than our proposed scheme. The comparison of our proposed scheme with WFCS illustrates that our proposed forwarded data aggregation scheme has a great impact on energy conservation. Furthermore, the comparison of our proposed scheme with the flooding scheme and TARA presented in Fig. 7b depicts that even for the increased densities of NBSs, the remaining energy is not substantially improved. TARA experiences the lowest remaining energy due to high data forwarding and packet retransmission rate that leads to the maximum consumption of energy resources.

5) COMPARISON OF TOTAL NUMBER OF ALIVE NBSs WITH THE INCREASING DENSITIES OF NBSs AND TCT OVER TIME

Fig. 8 illustrate that our proposed scheme results in the maximum number of alive NBSs for the increasing densities of NBSs (i.e., 100 and 150) at all the time instances. For both densities of NBSs, at time 0.5 seconds, for 30% TCT, our proposed scheme has almost 85% alive NBSs. While

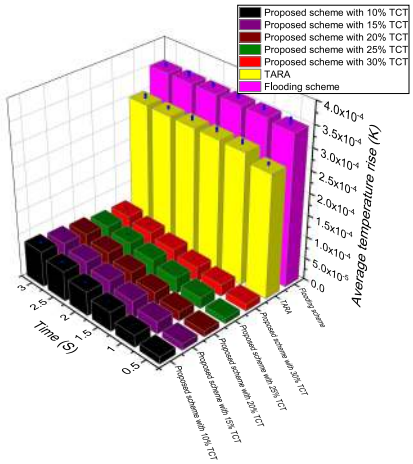

(a) Comparison of average temperature rise observed in our proposed scheme with the flooding scheme and TARA.

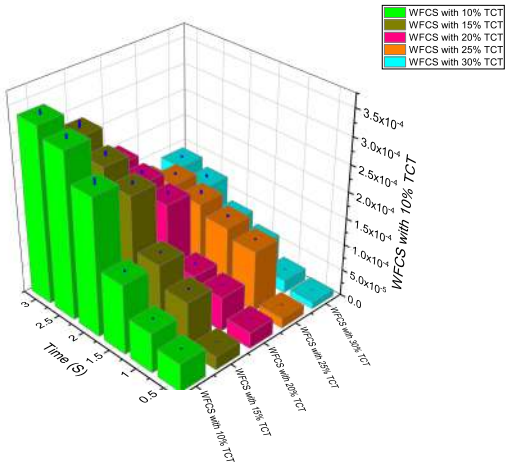

(b) Average temperature rise observed in WFCS.

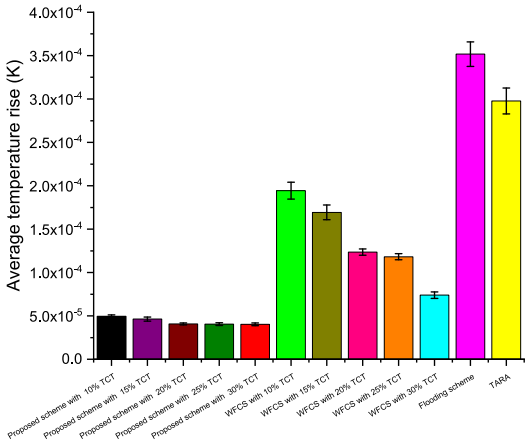

(c) Average temperature rise comparison at the end of simulations.

FIGURE 5. Average temperature rise comparison of our proposed scheme with WFCS, the flooding scheme and TARA with the density of 150 NBSs and increasing TCT over time.

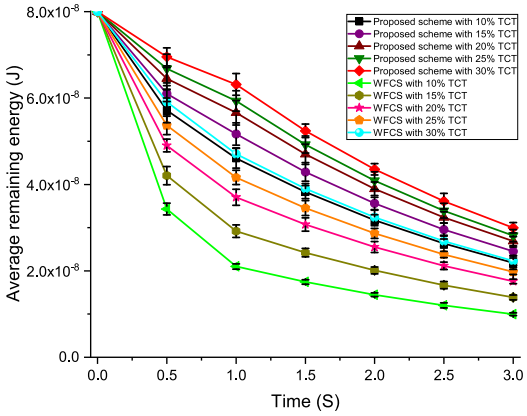

(a) Remaining energy comparison of our proposed scheme with WFCS.

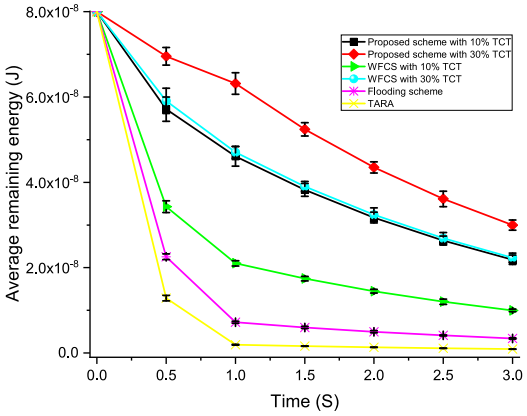

(b) Remaining energy comparison of our proposed scheme and WFCS with the flooding scheme and TARA.

FIGURE 6. Remaining energy comparison of our proposed scheme with WFCS, the flooding scheme and TARA with the density of 100 NBSs and increasing TCT over time.

for 10% TCT, almost 60% of NBSs are alive. WFDAS also results in a better alive number of NBSs as compared to the state-of-the-art-schemes. From Fig. 8b, we can see that the flooding scheme and TARA have the lowest number of alive NBSs. In TARA, NBSs died more rapidly due to monitoring of the neighboring NBSs and increased rate of packet

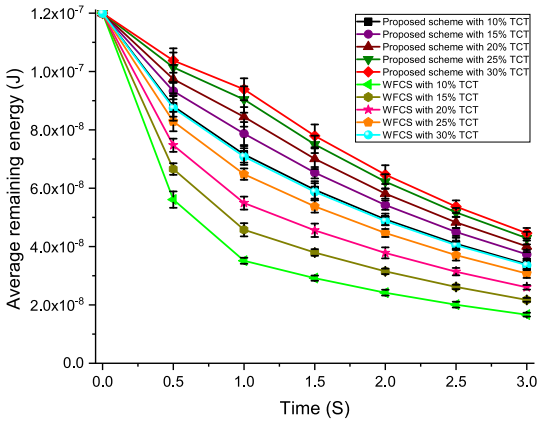

(a) Remaining energy comparison of our proposed scheme with WFCS.

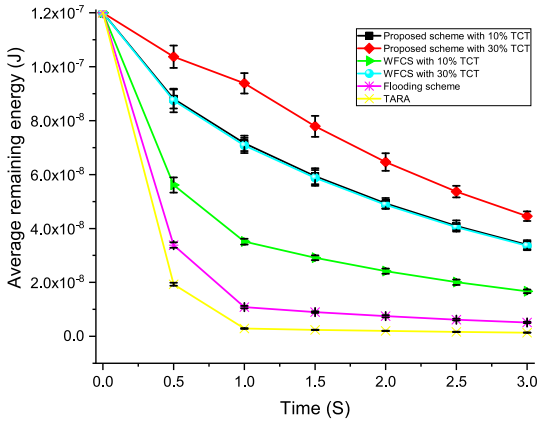

(b) Remaining energy comparison of our proposed scheme with WFCS, flooding scheme and TARA.

FIGURE 7. Remaining energy comparison of our proposed scheme with WFCS, the flooding scheme and TARA with the density of 150 NBSs and increasing TCT over time.

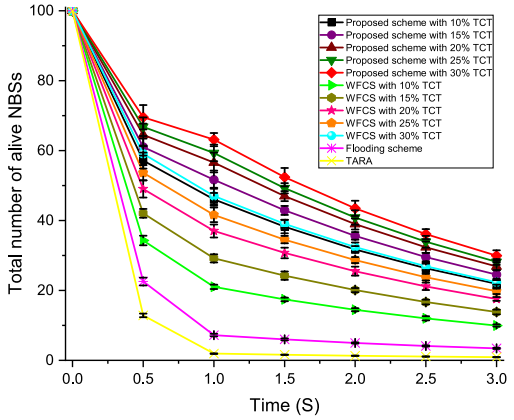

(a) Comparison of total number of alive NBSs with the density of 100 NBSs.

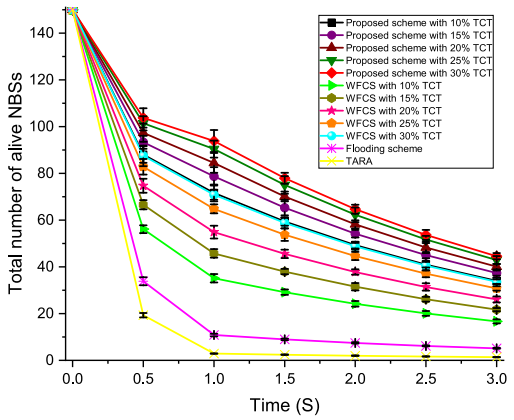

(b) Comparison of total number of alive NBSs with the density of 150 NBSs.

FIGURE 8. Comparison of total number of alive NBSs with WFCS, the flooding scheme and TARA for the increasing densities of NBSs and TCT over time.

retransmission for avoiding hotspots. From Fig. (8a,8b), we can observe that our controlled packet generation and efficient data forwarding strategy significantly increase the lifetime of NBSs.

6) COMPARISON OF TOTAL NOTIFICATIONS REPORTED IN OUR PROPOSED SCHEME WITH THE INCREASING DENSITIES AND TCT OVER TIME

Fig. 9 shows that when the TCT increases, the number of notifications reported by our proposed protocol decreases for the increasing densities of NBSs (i.e., 100 and 150). From Fig. 9a, we can see that when the NBSs density is 100 and TCT is 10%, maximum notifications are reported, whereas, for 30% the minimum number of notifications are reported. While the number of notifications in the flooding scheme and TARA remains fixed since all the reading detected by the NBSs are reported without any redundant data transmission control mechanism. Similarly, in Fig. 9b, we can see that the number of readings reported by our proposed scheme for the density of 150 is almost similar to the ones presented in Fig. 9a. This is because whenever the temporal correlation proportion is above the TCT, the data is notified. Therefore, for the lower value of TCT, our proposed scheme reports the maximum readings.

7) AVERAGE END-TO-END DELAY COMPARISON OF OUR PROPOSED SCHEME WITH THE INCREASING DENSITIES OF 100 AND 150 NBSs AND INCREASING TCT OVER TIME

From Fig. 10, we can observe that our proposed scheme experiences minimum average-end to-end delay for increasing densities of NBSs (i.e., 100 and 150) even at 10% TCT. The reason behind the negligible difference in the average end-to-end delay is the optimized selection of next-hop. Our proposed scheme experiences the lowest average end-to-end delay for 150 NBSs since when the NBSs density is increased, the number of potential next-hop NBSs also increases, which leads to reduced delay. Whereas, WFCS experiences more average end-to-end delay as compared to

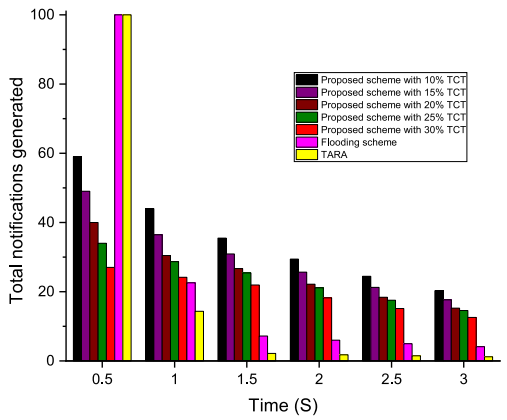

(a) Comparison of total notifications reported with the density of 100 NBSs.

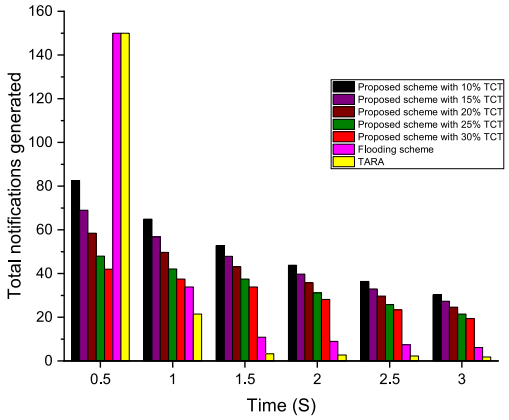

(b) Comparison of total notifications reported with the density of 150 NBSs.

FIGURE 9. Comparison of total notifications reported in our proposed scheme with the flooding scheme and TARA for the increasing densities of NBSs and increasing TCT over time.

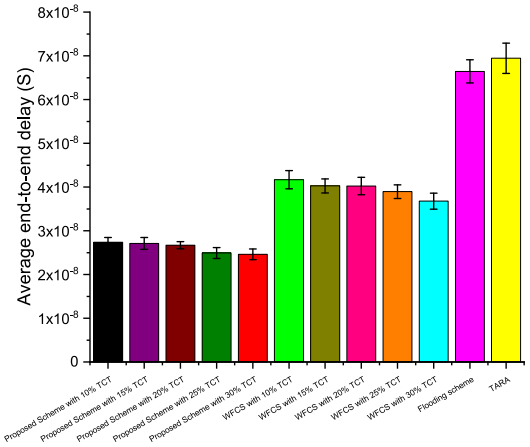

(a) Comparison of average end-to-end delay with the density of 100 NBSs.

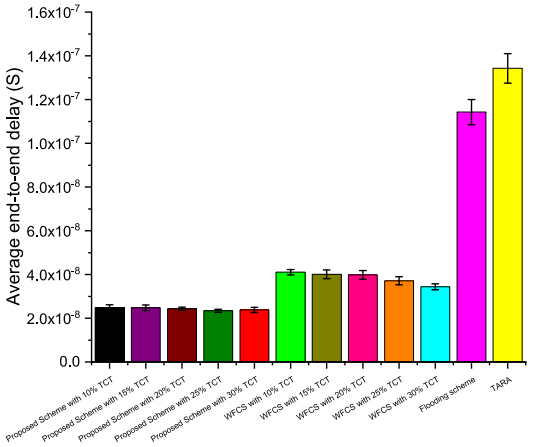

(b) Comparison of average end-to-end delay with the density of 150 NBSs.

FIGURE 10. Comparison of average end-to-end delay experienced in our proposed scheme with WFCS, the flooding scheme and TARA with the increasing densities of NBSs and TCT.

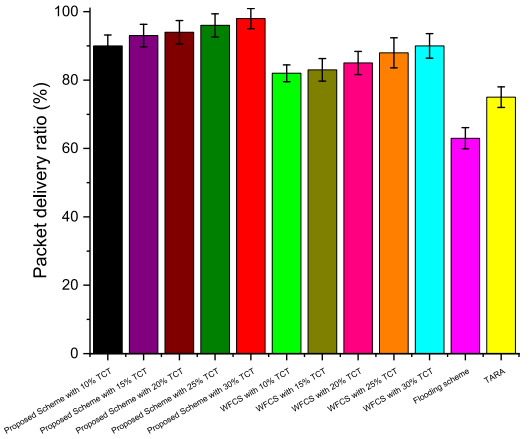

(a) Comparison of packet delivery ratio with the density of 100 NBSs.

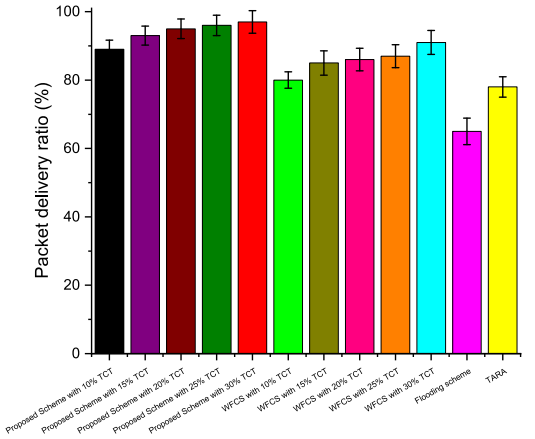

(b) Comparison of packet delivery ratio with the density of 150 NBSs.

FIGURE 11. Comparison of packet delivery ratio with WFCS, the flooding scheme and TARA with the increasing densities of NBSs and TCT.

our proposed scheme. The reason for the increased delay in WFCS is due to the forwarding of all packets without any aggregation at the intermediate NBS. Accordingly, the high packet forwarding rate ultimately leads to an increased average end-to-end delay. In the same manner, the flooding and TARA both show the maximum average end-to-end delay

for increasing densities of NBSs due to increased packet generation and forwarding rate.

8) PACKET DELIVERY RATIO COMPARISON OF OUR PROPOSED SCHEME WITH THE INCREASING DENSITIES OF 100 AND 150 NBSs AND INCREASING TCT OVER TIME

Fig. 11 visually compare the packet delivery ratio of our proposed scheme with WFCS, flooding and TARA schemes. From Fig. (11a,11b), it is evident that our proposed scheme achieve maximum packet delivery ratio for increasing density of NBSs. The high packet delivery ratio is due to minimum data congestion. Since WFCS transmits the forwarded packet without any suppression, therefore WFCS acheive almost 80% to 90% packet delivery ratio, which is still better than flooding and TARA scheme that have packet delivery ratio of less than 70% due to high data traffic.

In view of the detailed discussion of simulation results, it is evident that suppression of correlated data during data generation and data forwarding avoid transmission of redundant information and regulate data traffic under control. Therefore, our proposed strategy outperforms exiting schemes and results in controlled temperature rise, reduced end-to-end delay, improved network lifetime and packet delivery ratio.

V. CONCLUSION

The proposed routing protocol explicitly considers the feature and thermal challenges of IBNNs for designing a temperature-aware energy-efficient routing protocol for IBNNs. Furthermore, our proposed novel forwarded data aggregation approach combines forwarded packets to transmit only single to the destination for saving energy resources and avoiding antenna radiation exposure time. The obtained results confirm that our proposed approach reduces energy consumption and prevent temperature rise as compared to the state-of-the-art-schemes. In addition, our proposed strategy also avoids congestion and achieve low average end-to-end-delay. According to the comprehensive results and discussions, we conclude that our proposed protocol enables safer routing in terms of heat generation in a biological medium and improves the lifetime of an IBNN.

REFERENCES

[1] I. F. Akyildiz, F. Brunetti, and C. Blázquez, "Nanonetworks: A new communication paradigm," *Comput. Netw.*, vol. 52, no. 12, pp. 2260–2279, Aug. 2008.

[2] L. Yang and T. J. Webster, "Monitoring tissue healing through nanosensors," in *Nanotechnology Enabled in Situ Sensors for Monitoring Health*. New York, NY, USA: Springer, 2011, pp. 41–59.

[3] K. K. Jain, "Applications of nanobiotechnology in clinical diagnostics," *Clin. Chem.*, vol. 53, no. 11, pp. 2002–2009, Nov. 2007.

[4] I. F. Akyildiz, J. M. Jornet, and C. Han, "Terahertz band: Next frontier for wireless communications," *Phys. Commun.*, vol. 12, pp. 16–32, Sep. 2014.

[5] Y. J. Heo and S. Takeuchi, "Towards smart tattoos: Implantable biosensors for continuous glucose monitoring," *Adv. Healthcare Mater.*, vol. 2, no. 1, pp. 43–56, Jan. 2013.

[6] S. Agrawal and R. Prajapati, "Nanosensors and their pharmaceutical applications: A review," *Int. J. Pharm. Sci. Technol.*, vol. 4, pp. 1528–1535, Mar. 2012.

[7] M. A. Eckert, P. Q. Vu, K. Zhang, D. Kang, M. M. Ali, C. Xu, and W. Zhao, "Novel molecular and nanosensors for *in vivo* sensing," *Theranostics*, vol. 3, no. 8, pp. 583–594, 2013.

[8] I. F. Akyildiz and J. M. Jornet, "Electromagnetic wireless nanosensor networks," *Nano Commun. Netw.*, vol. 1, no. 1, pp. 3–19, Mar. 2010.

[9] G. Piro, G. Boggia, and L. A. Grieco, "On the design of an energy-harvesting protocol stack for body area nano-NETworks," *Nano Commun. Netw.*, vol. 6, no. 2, pp. 74–84, Jun. 2015.

[10] F. Afsana, M. Asif-Ur-Rahman, M. R. Ahmed, M. Mahmud, and M. S. Kaiser, "An energy conserving routing scheme for wireless body sensor nanonetwork communication," *IEEE Access*, vol. 6, pp. 9186–9200, 2018.

[11] H. Fahim, W. Li, S. Javaid, M. M. Sadiq Fareed, G. Ahmed, and M. K. Khattak, "Fuzzy logic and bio-inspired firefly algorithm based routing scheme in intrabody nanonetworks," *Sensors*, vol. 19, no. 24, p. 5526, 2019.

[12] J. Xu, Y. Zhang, J. Jiang, and J. Kan, "An energy balance clustering routing protocol for intra-body wireless nanosensor networks," *Sensors*, vol. 19, no. 22, p. 4875, 2019.

[13] G. Piro, K. Yang, G. Boggia, N. Chopra, L. A. Grieco, and A. Alomainy, "Terahertz communications in human tissues at the nanoscale for healthcare applications," *IEEE Trans. Nanotechnol.*, vol. 14, no. 3, pp. 404–406, May 2015.

[14] J. M. Jornet and I. F. Akyildiz, "Channel modeling and capacity analysis for electromagnetic wireless nanonetworks in the terahertz band," *IEEE Trans. Wireless Commun.*, vol. 10, no. 10, pp. 3211–3221, Oct. 2011.

[15] H. Elayan, R. M. Shubair, J. M. Jornet, and R. Mittra, "Multi-layer intrabody terahertz wave propagation model for nanobiosensing applications," *Nano Commun. Netw.*, vol. 14, pp. 9–15, Dec. 2017.

[16] J. Kokkoniemi, J. Lehtomäki, and M. Juntti, "A discussion on molecular absorption noise in the terahertz band," *Nano Commun. Netw.*, vol. 8, pp. 35–45, Jun. 2016.

[17] R. Zhang, K. Yang, A. Alomainy, Q. H. Abbasi, K. Qaraqe, and R. M. Shubair, "Modelling of the terahertz communication channel for *in-vivo* nano-networks in the presence of noise," in *Proc. 16th Medit. Microw. Symp. (MMS)*, Nov. 2016, pp. 1–4.

[18] H. Elayan, P. Johari, R. M. Shubair, and J. M. Jornet, "Photothermal modeling and analysis of intrabody terahertz nanoscale communication," *IEEE Trans. Nanobiosci.*, vol. 16, no. 8, pp. 755–763, Dec. 2017.

[19] S. Javaid, Z. Wu, H. Fahim, F. Javed, and J. Chen, "Analyzing the impact of nanonode density on biological tissues in intrabody nanonetworks," in *Proc. Int. Conf. Netw. Netw. Appl. (NaNA)*, Oct. 2018, pp. 159–163.

[20] C. Oey and S. Moh, "A survey on temperature-aware routing protocols in wireless body sensor networks," *Sensors*, vol. 13, no. 8, pp. 9860–9877, 2013.

[21] S. Movassaghi, M. Abolhasan, and J. Lipman, "A review of routing protocols in wireless body area networks," *J. Netw.*, vol. 8, no. 3, pp. 559–575, 2013.

[22] S. Sarkar and S. Misra, "From micro to nano: The evolution of wireless sensor-based health care," *IEEE Pulse*, vol. 7, no. 1, pp. 21–25, Jan. 2016.

[23] H. Fahim, W. Li, S. Javed, and F. Javed, "Bio-inspired nanorouter mobility model for energy efficient data collection in intrabody nanonetwork," in *Proc. Int. Conf. Netw. Netw. Appl. (NaNA)*, Oct. 2019, pp. 124–128.

[24] S. Javaid, H. Fahim, X. Liao, and F. Javed, "Exploiting temporal correlation mechanism for energy efficient data collection in intrabody nanonetworks," in *Proc. Int. Conf. Netw. Netw. Appl. (NaNA)*, Oct. 2019, pp. 119–123.

[25] H. Elayan, R. M. Shubair, J. M. Jornet, and P. Johari, "Terahertz channel model and link budget analysis for intrabody nanoscale communication," *IEEE Trans. Nanobiosci.*, vol. 16, no. 6, pp. 491–503, Sep. 2017.

[26] G. Piro, L. A. Grieco, G. Boggia, and P. Camarda, "Nano-sim: Simulating electromagnetic-based nanonetworks in the network simulator 3," in *Proc. 6th Int. Conf. Simulation Tools Techn.*, 2013, pp. 203–210.

[27] S. Canovas-Carrasco, A.-J. Garcia-Sanchez, and J. Garcia-Haro, "A nanoscale communication network scheme and energy model for a human hand scenario," *Nano Commun. Netw.*, vol. 15, pp. 17–27, Mar. 2018.

[28] Q. Tang, N. Tummala, S. K. Gupta, and L. Schwiebert, "Tara: Thermal-aware routing algorithm for implanted sensor networks," in *Proc. Int. Conf. Distrib. Comput. Sensor Syst.* Marina del Rey, CA, USA: Springer, 2005, pp. 206–217.

[29] D. Takahashi, Y. Xiao, and F. Hu, "LTRT: Least total-route temperature routing for embedded biomedical sensor networks," in *Proc. IEEE GLOBECOM Global Telecommun. Conf.*, Nov. 2007, pp. 641–645.

[30] A. Bag and M. A. Bassiouni, "Hotspot preventing routing algorithm for delay-sensitive biomedical sensor networks," in *Proc. IEEE Int. Conf. Portable Inf. Devices*, May 2007, pp. 1–5.
[31] A. Bag and M. A. Bassiouni, "Routing algorithm for network of homogeneous and id-less biomedical sensor nodes (RAIN)," in *Proc. IEEE Sensors Appl. Symp.*, Feb. 2008, pp. 68–73.
[32] A. R. Bhangwar, A. Ahmed, U. A. Khan, T. Saba, K. Almustafa, K. Haseeb, and N. Islam, "WETRP: Weight based energy & temperature aware routing protocol for wireless body sensor networks," *IEEE Access*, vol. 7, pp. 87987–87995, 2019.
[33] A. O. Govorov, W. Zhang, T. Skeini, H. Richardson, J. Lee, and N. A. Kotov, "Gold nanoparticle ensembles as heaters and actuators: Melting and collective plasmon resonances," *Nanosc. Res. Lett.*, vol. 1, no. 1, pp. 84–90, Nov. 2006.
[34] H. H. Richardson, M. T. Carlson, P. J. Tandler, P. Hernandez, and A. O. Govorov, "Experimental and theoretical studies of Light-to-Heat conversion and collective heating effects in metal nanoparticle solutions," *Nano Lett.*, vol. 9, no. 3, pp. 1139–1146, Mar. 2009.
[35] M. Richard M. Bergenstal. (2018). *Understanding Continuous Glucose Monitoring Data Role of Continuous Glucose Monitoring in Diabetes Treatment*. Arlington, VA, USA: American Diabetes Association. [Online]. Available: https://www.ncbi.nlm.nih.gov/books/NBK538967/, doi: 10.2337/db20181-20
[36] J. M. Jornet and I. F. Akyildiz, "Femtosecond-long pulse-based modulation for Terahertz band communication in nanonetworks," *IEEE Trans. Commun.*, vol. 62, no. 5, pp. 1742–1754, May 2014.
[37] J. M. Jornet, "A joint energy harvesting and consumption model for self-powered nano-devices in nanonetworks," in *Proc. IEEE Int. Conf. Commun. (ICC)*, Jun. 2012, pp. 6151–6156.

SHUMAILA JAVAID received the B.S. degree from COMSATS University Islamabad (CUI), Pakistan, in 2012, and the M.S. degree in telecommunication and networking from Bahria University, Pakistan, in 2015. She is currently pursuing the Ph.D. degree in computer science with Shaanxi Normal University, China. Her main research interests include wireless sensor and wireless multimedia sensor networks, intrabody nanonetworks, information centric networks, and wireless networking in general.

ZHENQIANG WU received the B.S. degree from Shaanxi Normal University, China, in 1991, and the M.S. and Ph.D. degrees from Xidian University, China, in 2002 and 2007, respectively. He is currently a Full Professor with Shaanxi Normal University. His research interests include computer communications networks, mainly wireless networks, network security, anonymous communication, and privacy protection. He is a member of ACM and Senior of CCF.

HAMZA FAHIM received the B.S. and M.S. degrees from the Computer Science Department, COMSATS University Islamabad (CUI), Pakistan, in 2012 and 2015, respectively. He is currently pursuing the Ph.D. degree in computer science and networks with the School of Electronics and Information Technology, Xi'an Jiaotong University, China. His current research interests include intrabody nanonetworks, software defined networks, and wireless sensor networks.

MIAN MUHAMMAD SADIQ FAREED received the Ph.D. degree in communication and information engineering from the School of Electronic and Information Engineering, Xi'an Jiaotong University, Xi'an, China. He is currently working as an Associate Professor with the Guilin University of Technology, Guilin, China. His research interests include computer vision, object detection/segmentation, wireless body area networks, and wireless sensor networks.

FARHANA JAVED received the bachelor's degree from COMSATS University, in 2016, and the master's degree in computer applied technology from the Huazhong University of Science and Technology (HUST), Wuhan, China, in 2019. She is currently pursuing the Ph.D. degree with the Universitat Politècnica de Catalunya (UPC), Barcelona. She is currently a Research Assistant with the Communication Networks Division, Centre Tecnològic de Telecomunicacions de Catalunya (CTTC). Her current research interests include software-defined networks and network functions virtualization applied to mobile networks, the Internet of NanoThings, and intrabody area nanonetworks.